Journal of Fluids and Structures (2002) **16**(5), 613–626
doi:10.1006/jfls.437 available online at http://www.idealibrary.com on IDEAL®

ACTIVE STABILIZATION OF A PLANAR JET IMPINGING ON A FLEXIBLE WEDGE

S. Ziada

Department of Mechanical Engineering, McMaster University
Hamilton, Ontario, L8S 4L7, Canada

(Received 29 August 2000; accepted in revised form 4 June 2001)

Feedback control is used to suppress the "*lock-in*" vibration and the pressure pulsation generated by an unstable planar jet impinging upon a *flexible* wedge (or edge). First, the lock-in vibration to be controlled is shown to be caused by the coupling between a robust "*jet-edge oscillator*" and a resonant vibration mode of the wedge. Since the system oscillation is controlled by the resonant response of the wedge, the frequency of oscillation within the lock-in range can deviate substantially from the natural frequency of the "jet-edge oscillator". In order to counteract the upstream effect resulting from the *wedge vibration*, an adaptive digital controller is used to activate loudspeakers focused on the jet exit. The paper describes the system response as the lock-in vibration is gradually suppressed. When the *vibration signal* was used to activate the controller, the edge vibration was substantially reduced, but the jet oscillation switched to the natural oscillation mode of the jet-edge oscillator, resulting in only a slight reduction in the pressure amplitude. However, when the *pressure signal* was used to activate the controller, the vibrations and pressure oscillations were entirely suppressed without destabilizing other modes of the system.

1. INTRODUCTION

Self-excited flow oscillations are often encountered in many engineering applications involving internal or external flows. The resulting pressure pulsations and structural vibrations can reduce the process efficiency, generate unacceptable noise levels and, in some cases, cause fatigue failure to the associated equipment. Self-excited flow oscillations have been reported for piping systems conveying gases or liquids, flow control devices, turbomachines, tube bundles, combustion chambers, cavities in moving vehicles, and many other industrial, aeronautical and marine applications. In many of these examples, global flow oscillations are generated by an excitation mechanism which couples a convectively unstable free shear flow (e.g. jets and free shear layers) with an upstream feedback effect resulting from either flow impingement or system resonance. In the former case, upstream feedback results from the distortion of the vorticity field associated with flow impingement on downstream objects, whereas in the latter, the pressure field generated by the acoustic or structural resonator provides it. This upstream feedback is the most crucial event of the excitation mechanism because it perpetuates the inducement of new perturbations, and thereby sustains the global oscillations at selected discrete frequencies. Excellent reviews of these excitation mechanisms can be found in Rockwell & Naudascher (1979) and Naudascher & Rockwell (1994). This paper focuses on the case when the global oscillations are sustained by an upstream effect due to structural resonance.

0889-9746/02/050613 + 14 $35.00/0

Active control of global flow oscillations has received considerable attention in recent years. Several authors employed external excitations at prescribed frequencies and amplitudes with the objective of disturbing or modulating the global mode of oscillation, and thereby reduce its intensity or alter its frequency [see, for example, Rockwell (1992), Nakano & Rockwell (1993), Wiltse & Glezer (1993), Gopalkrishnan et al. (1994), among others]. For the case of flow-excited resonance, very promising results of *feedback control* have been published. Ffowcs Williams & Huang (1989), Baz & Ro (1991), Huang & Weaver (1991) and Welsh et al. (1991) have used loudspeakers or electromagnetic exciters, which were activated by the signal of system oscillation, in order to counteract the response of the resonator and thereby suppress the resonant oscillations. More recently, Ziada (1995) used an alternative approach by focusing loudspeakers on the most receptive region of the flow, which is at the location of flow separation. By means of an adaptive digital controller, Ziada has shown that the *very robust oscillations* of the jet-edge and jet-slot oscillators can be effectively suppressed without destabilizing other modes. This was achieved in the absence of any resonance effects.

Active suppression of shallow cavity acoustic resonance has also been demonstrated, with varying degrees of success, by means of perturbing the shear layer at its separation location with the aid of oscillating flaps (McGrath & Shaw 1996), pulsed mass injection (Sarno & Franke 1994) or piezoelectric actuators (Cattafesta et al. 1997). In these studies, however, since the resonance was excited by a turbulent grazing flow, suppression of the acoustic resonant modes did not destabilize other modes corresponding to the natural oscillation modes of the impinging shear flow. This is because impinging turbulent shear layers do not generally exhibit strong discrete frequency oscillations in the absence of resonance effects.

In a recent study (Ziada 1999), the effect of feedback control on the acoustic resonance of two coaxial deep cavities excited by *a jet-slot oscillator* has been investigated. In this case, the jet-slot oscillator can generate strong oscillation even in the absence of acoustic resonances (Ziada 1995). Thus, when the acoustic resonant oscillations were actively suppressed, the system reverted to the natural oscillation mode of the jet-slot oscillator, whose frequency and pattern of jet oscillation are distinctively different from those occurring at acoustic resonant oscillations (Ziada 2001). It was therefore suggested that better control could be achieved by employing multiple controllers and speakers in order to simultaneously attenuate both the acoustic resonance and the jet-slot oscillations.

The present paper considers the effect of feedback control on the *lock-in* oscillation exhibited by a planar jet impinging upon a flexible wedge. As in the acoustic resonance case mentioned above (Ziada 2001), even in the absence of the resonant wedge vibration, the system still constitutes a strong jet-edge oscillator (Powell 1961). However, when the wedge vibration amplitude becomes large, it starts to control the oscillation frequency, and therefore this frequency could deviate substantially from that of the natural jet-edge oscillations.

The feedback control concept employed in this work is similar to that described by Ziada (1995) and is illustrated in Figure 1. The figure shows the block diagram of the excitation mechanism, together with the "*active control feedback*", which is added to counteract the self-generated feedback. In the present case, the active feedback can be developed from either the wedge vibration signal or from the signal of the pressure pulsation. As will be shown in this paper, the choice of the signal which activates the controller has a crucial effect on the performance of the feedback control technique.

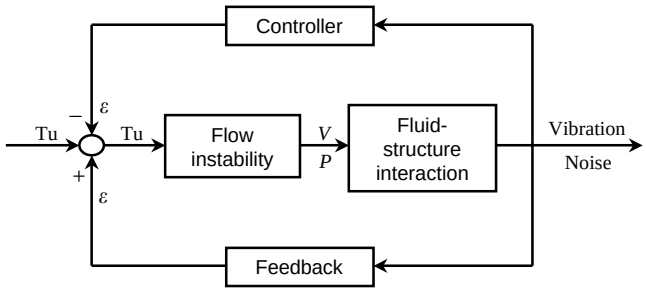

Fig. 1. Block diagram representation of the feedback mechanism causing lock-in vibrations and the basic idea to suppress this mechanism by active means. Tu is the broadband flow turbulence, V and P are the velocity and pressure fluctuations, and ε is the upstream feedback.

2. EXPERIMENTAL TECHNIQUE

The experimental set-up consisted of a two-dimensional jet impinging upon an edge, i.e. the so-called "jet-edge oscillator". This flow configuration is known to generate strong global oscillation in the absence of resonance effects (Powell 1961). However, the edge (or the wedge) was made flexible to promote resonant vibration of the wedge excited by the jet-edge oscillator. As shown in Figure 2, a 450 mm long air nozzle exhausting into a large anechoic chamber supplied a two-dimensional (planar) jet. Three loudspeakers were mounted at each side of the nozzle exit. The three speakers at one side of the nozzle were connected in series to form one set of speakers. The two sets of speakers were then connected to operate out-of-phase with each other in order to be able to impose antisymmetric excitation at the jet exit. Aluminium plates, 5 mm in thickness, were used to cover the speakers and the side gaps were sealed except those towards the nozzle lip such that the excitation by the speakers was focused on the nozzle exit only. Additional details regarding the loudspeakers and the cover plates can be found in Ziada (1995).

The impingement edge was constructed of a small 30° wooden wedge, which was mounted on two cantilever beams made of spring steel. Numerous preliminary tests were carried out to tune the system and generate lock-in vibration over a wide velocity range. In the lock-in range, the system oscillation frequency does not change with the flow velocity, but remains constant at the resonance frequency of the wedge. The preliminary tests included changing the jet thickness, the impingement length and the stiffness of the cantilever springs. An optimum set-up was obtained when the jet thickness was 14 mm, the impingement length was 63 mm and the cantilever springs had a length of 60 mm and cross-section dimensions of 3 mm × 15 mm. The resonance frequencies of the wedge were found to be 110 Hz for the translation mode, and 142 Hz for the rocking mode. A strobe light was employed to determine these vibration modes.

The flow velocity at the nozzle was calculated from the measured pressure drop at the nozzle. Dantec type hot wire anemometer and linearizer were used to measure the mean velocity profile and the velocity fluctuations. As shown in Figure 2, the pressure fluctuation was recorded by means of a condenser microphone which was positioned at 10 cm distance from the tip of the wedge, and the wedge vibration was measured with the aid of two small accelerometers attached to the cantilever springs. All signals were analysed with the aid of a four-channel spectrum analyser.

Two different types of controllers were used in this study. The first was an analogue controller, consisting of a general-purpose analogue filter, an in-house made phase shifter and a power amplifier. This controller had to be adjusted manually until the optimal

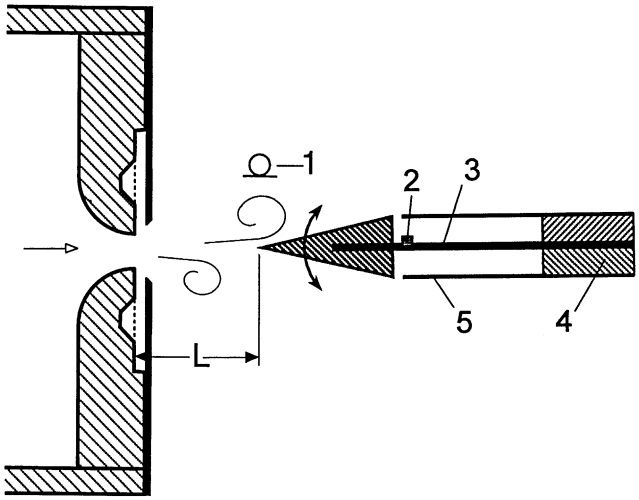

Fig. 2. Experimental set-up illustrating a two-dimensional jet impinging on a flexible wedge. 1: microphone; 2: accelerometer; 3: two cantilevered springs; 4: rigid support; 5: cover plates.

settings were attained. Alternatively, a commercial digital controller type Digisonix dx-57 was employed instead of the filter and the phase shifter. Although this controller was developed for active noise cancellation applications, which require a clear input reference signal, it performed remarkably well in the present tests, in which the reference input signal practically vanishes when the system becomes under control. This controller employs an IIR digital filter whose coefficients are optimized by means of a recursive root-mean-square algorithm. Either the signal of the wedge vibration or that of the pressure pulsation could be used to activate the controller. In the digital control case, the same signal was used as the input reference signal and also as the error signal.

The flow was visualized by injecting smoke into the nozzle at 15 cm upstream of its exit. The smoke remained in the jet shear layers and visualized clearly the jet development with and without feedback control. A strobe light, activated by the pressure or the vibration signal, was used to slow the jet oscillation, which was then recorded on a video system. A video mixer and a second camera were used to superimpose the vibration and pressure signals on the visualized flow field. More details of the flow visualization technique can be found in Ziada (1995).

3. OVERVIEW OF SYSTEM OSCILLATIONS

3.1. Effect of Wedge Resonance on the Jet-Wedge Oscillator

Figure 3 shows three pairs of vibration and pressure spectra for three selected values of flow velocity. The first pair corresponds to a flow velocity at which the frequency of the jet-edge oscillator is just below that of the wedge resonance. The second pair, Figure 3(b), represents typical spectra within the lock-in range. It is interesting to note that despite the sharp increase in the vibration amplitude (more than an order of magnitude) the amplitude of the pressure fluctuations does not increase so sharply; it increases by a factor which is smaller than three. This is due to the fact that the "jet-rigid edge" by itself is a strong source of pressure oscillations. It also pinpoints the strong non-linear character of

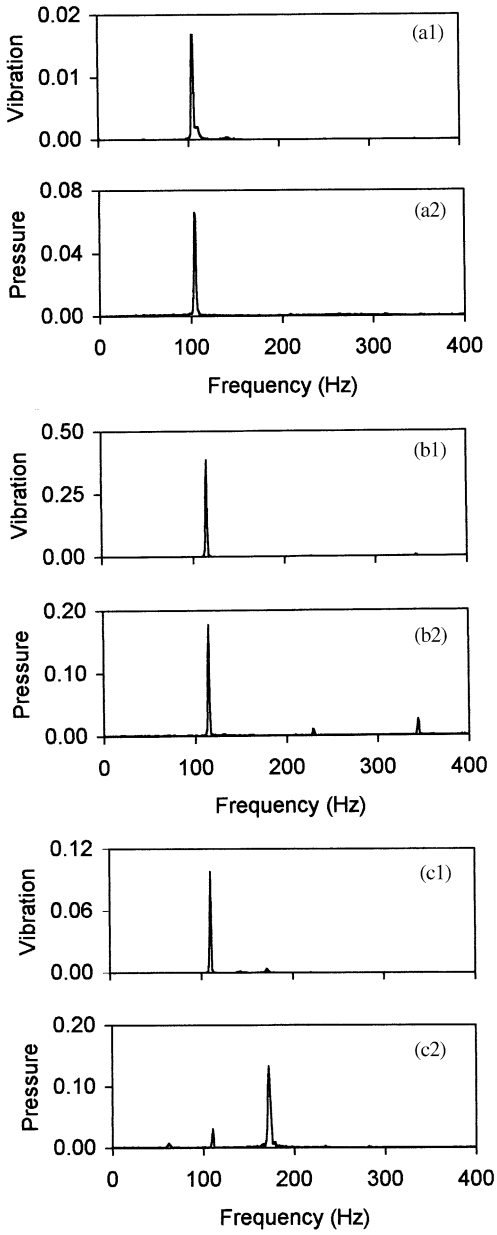

Fig. 3. Typical vibration and pressure spectra taken at different flow velocities within the lock-in range of the wedge vibration. All units are relative. Flow velocity: (a) $V = 16{\cdot}5\,\text{m/s}$; (b) $V = 19\,\text{m/s}$; (c) $V = 28{\cdot}2\,\text{m/s}$.

disturbance amplification in the impinging jet. For a mixing layer impinging on a rigid wedge, Ziada & Rockwell (1982) showed that the maximum amplitude of velocity fluctuation at the wedge is insensitive to the initial disturbance amplitude at the separation location.

Similar features can be seen in Figure 3(c), which corresponds to a flow velocity beyond the lock-in range, that is when the jet-edge oscillator detaches itself from the wedge resonant response. As can be seen, the pressure oscillations occur predominantly at

175 Hz, whereas the wedge still vibrates at 110 Hz. Here again, the amplitude of the pressure pulsation does not decrease much as the resonant (or the lock-in) vibration subsides, which is indicative of the strength of jet-edge oscillations, even in the absence of wedge resonance.

3.2. Overall System Response

The overall system response as a function of the flow velocity was studied by means of pressure and vibration spectra such as those presented in Figure 3. However, it was rather difficult to complete this task because the amplitude of wedge vibration was so large (approximately $\pm$ 5 mm) that the cantilever springs broke several times during the initial experiments to characterise the system response. Since it was not possible to reproduce accurately the same system response after replacing the springs, the measurements had to be repeated from the start every time a spring was broken. *In fact, it would not have been possible to complete this study, had active control not been used at the outset of the experiments to reduce the vibration amplitude during the tests*. In other words, when the data acquisition of each large-amplitude vibration case was completed, the controller was promptly activated to suppress the wedge vibration during the idle running time while the results were being inspected, stored and transferred. In this way, the lifetime of the cantilever springs was sufficiently extended until the experiments were completed.

Another approach to solve the problem of spring failure would have been to use stiffer springs and a heavier wedge, so that the wedge frequency remains within the desired range. However, this would have resulted in smaller vibration amplitudes and thereby narrower range of lock-in. Such effects were not desired because the main focus was to study the effect of feedback control on a strong lock-in case of fluid–structure interaction.

Figure 4 shows the details of the system response as the flow velocity is increased from 8 to 35 m/s. Figures 4(a) and 4(b) depict the frequencies of the wedge vibration and the pressure pulsation, respectively, and Figures 4(c) and 4(d) show the normalized amplitudes of wedge vibration and pressure pulsation. The wedge vibration is normalized by using the spring stiffness (K), the dynamic head ($\frac{1}{2}\rho V^2$) and the area of the wedge (S), whereas the pressure amplitude is normalized by the dynamic head. Thus, the normalized amplitudes for the wedge vibration, ϕ, and the pressure, P, are given by:

$$\phi = \frac{A_{\mathrm{rms}} K}{\frac{1}{2}\rho V^2 S}, \tag{1}$$

$$P = \frac{P_{\mathrm{rms}}}{\frac{1}{2}\rho V^2}, \tag{2}$$

where $A_{\mathrm{r.m.s.}}$ and $P_{\mathrm{r.m.s.}}$ are the root-mean-square amplitudes of wedge vibration and pressure pulsation, respectively. Different data points in Figure 4 indicate whether the flow velocity of the jet, V, is being increased or decreased. This does not seem to produce any noticeable hysteresis in the lock-in range. However, the maximum amplitudes are higher when the flow velocity is being decreased.

As shown in Figures 4(a) and 4(b), the lock-in range starts at a flow velocity near 15 m/s, where the wedge oscillation frequency is seen to drop to the frequency of the jet-edge oscillation (i.e. from 110 to 98 Hz). The lock-in range ends near 26 m/s, at which the pressure oscillation is seen to separate from the wedge resonance frequency. Within the lock-in range, the frequency of pressure pulsation, i.e. the jet oscillation frequency, is controlled by the wedge vibration at its resonance frequency near 110 Hz. Outside the lock-in range, the frequency of pressure pulsation follows a constant Strouhal number

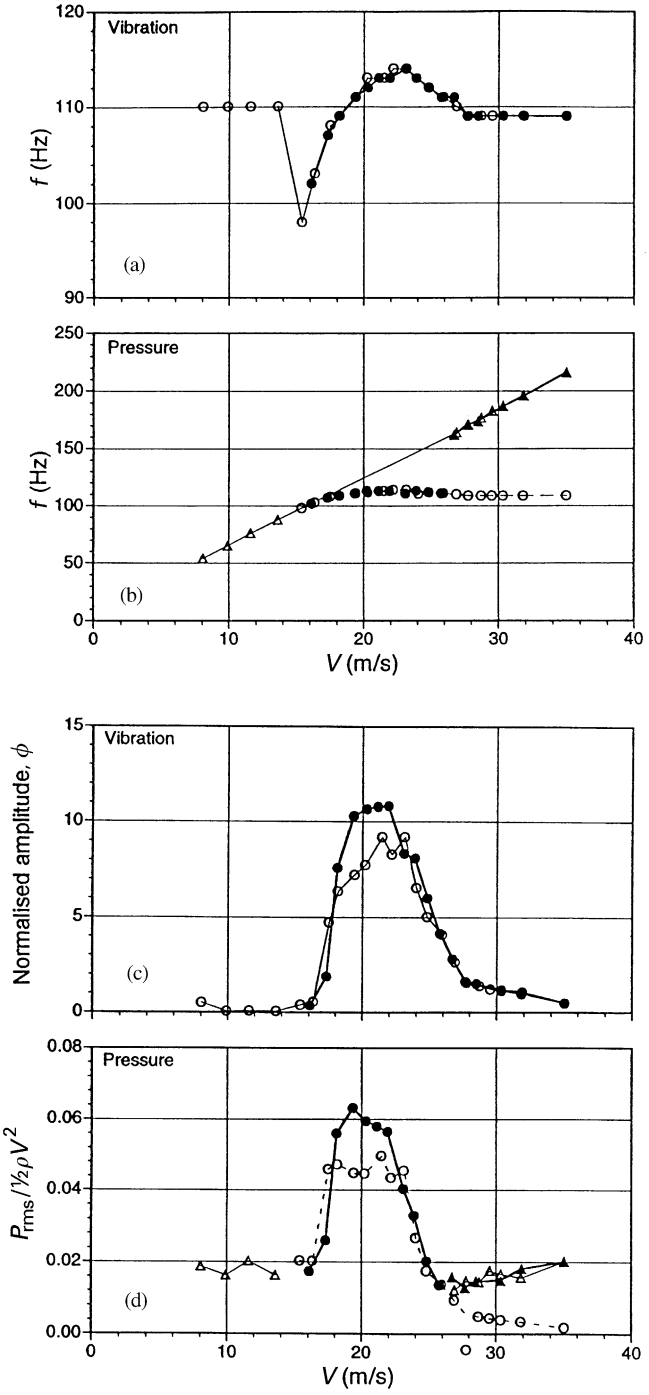

Fig. 4. Response characteristics of the system. (a) Frequency of wedge vibration; (b) frequency of pressure oscillation; (c) normalized amplitude of wedge vibration; (d) normalized amplitude of pressure oscillation: ○, ●, Oscillations at wedge frequency; Δ, ▲, frequency of natural jet-edge oscillation; open points, increasing velocity, filled points, decreasing velocity.

relationship, indicating that the jet is oscillating at the natural mode of the jet-wedge oscillator. As illustrated in Figures 4(c) and 4(d), the vibration amplitude increases drastically within the lock-in range, but the amplitude of the pressure pulsation increases only moderately.

Figure 5 shows flow visualization photographs of a typical oscillation cycle within the lock-in range. The top signal in these photographs corresponds to the wedge vibration and the bottom signal represents the pressure pulsation at 10 cm from the tip of the wedge. Photograph 5(b) corresponds to the maximum downward displacement of the wedge, whereas the wedge is at its maximum upward location in Photograph 5(d).

From the proceeding discussions, it is clear that there are two excitation mechanisms which "compete" for dominance: the jet-edge mechanism with fluid-dynamic feedback and the resonant mechanism with structural resonance feedback. Within the lock-in range, the oscillation (or resonant) frequency is clearly different from the frequency of the jet-edge natural oscillation. The object of the next section is to gain more insight into how the system reacts when active control is applied to suppress the resonant vibration within the lock-in range.

4. RESULTS OF FEEDBACK CONTROL

As mentioned earlier, two different controllers have been employed to understand the system response to feedback control. First the results of the narrow band (or analogue)

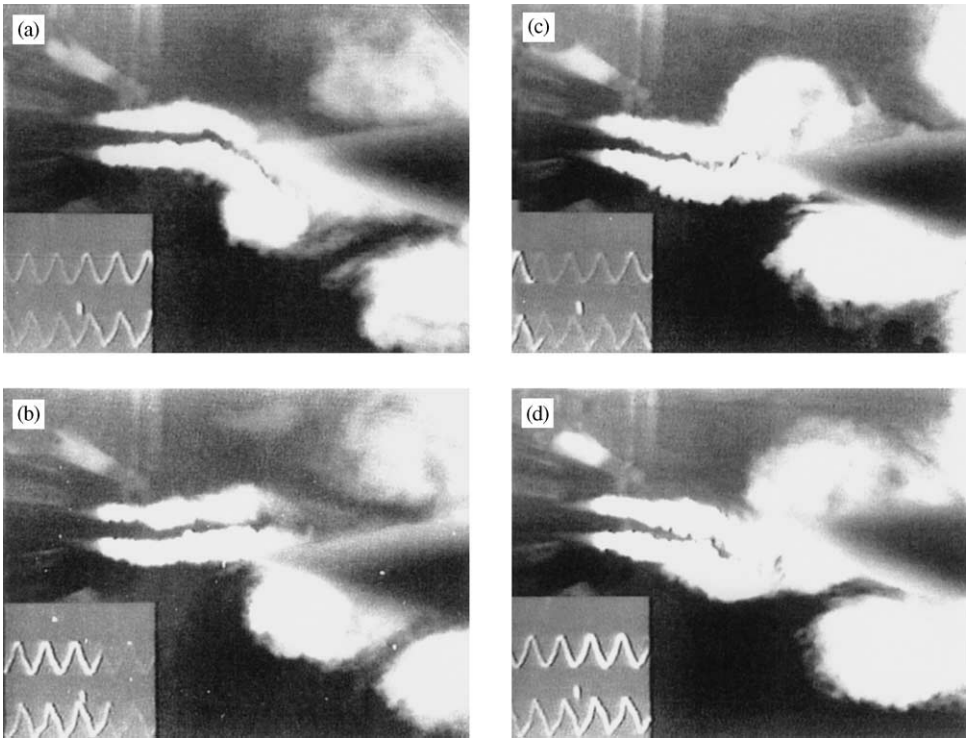

Fig. 5. Flow visualization photographs showing one oscillation cycle of the lock-in wedge vibration. $V = 21$ m/s.

controller will be discussed and, thereafter, those of the adaptive digital controller are addressed. Attention will be focussed on the lock-in range only.

4.1. Results of the Narrow-Band Controller

The narrow-band controller consisted of a filter, followed by a phase shifter and a power amplifier. By means of this set-up, the phase of the feedback signal activating the loudspeakers can be properly adjusted over a very narrow frequency range centred on the system oscillation frequency.

The effect of the narrow band controller is illustrated in Figure 6, which shows spectra of wedge vibration and pressure oscillation without and with control. The three cases presented correspond to test conditions near the beginning, the middle and the end of the lock-in range. *The vibration signal was used to activate the speakers in the three cases*. The spectra shown in Figure 6 represent the cases of maximum vibration reduction by means of optimal adjustments of both the phase shift and the gain of the narrow band controller.

At $V \approx 18$ m/s, i.e. at the beginning of the lock-in range (Figure 4), the vibration amplitude is relatively small. Despite the smallness of this amplitude, the narrow-band controller reduced the vibration and the pressure amplitudes by an amount of approximately 10 dB. Near the middle and the end of the lock-in range, $V = 21$ and 23·5 m/s, the vibration amplitude is rather large, as shown in Figure 4. The narrow-band controller reduced the vibration amplitude drastically, by more than 30 dB, but had little effect on the pressure amplitude (as can be seen by comparing the upper with the lower spectra in Figure 6). *Similarly to the case of flow-excited acoustic resonance (Ziada 1999), the system oscillation simply switched to a higher frequency approximating the natural frequency of the jet-'rigid' edge oscillator,* which could not be controlled by this type of controller.

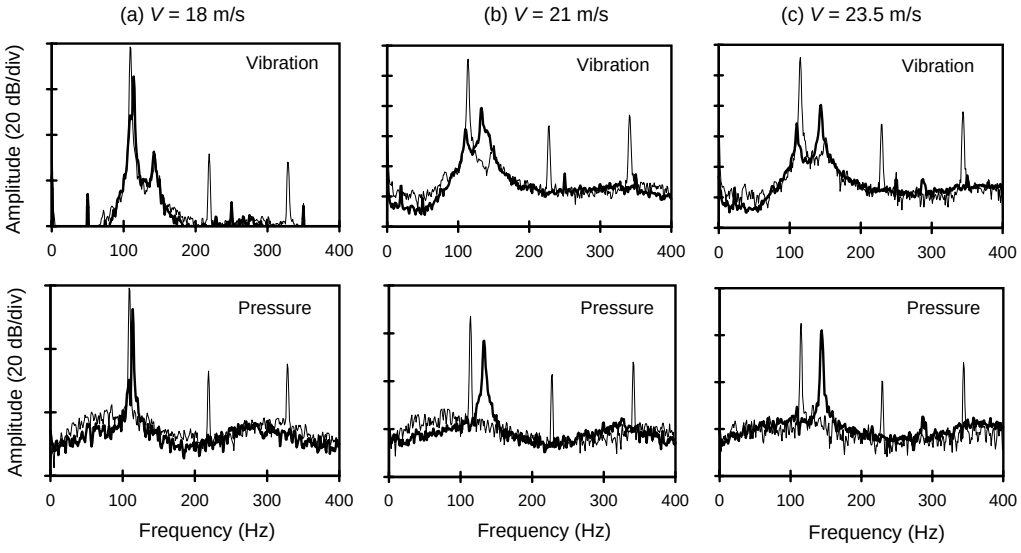

Fig. 6. Effect of the narrow-band controller on the lock-in wedge vibration. The three cases correspond to test conditions within the lock-in range. Upper spectra: wedge vibration; lower spectra: pressure oscillations. (a) $V = 18$ m/s; (b) 21 m/s; (c) 23·5 m/s. *The vibration signal activated the controller*.

4.2. Results of the Adaptive Digital Controller

First, as in the previous case, the signal of the wedge vibration was used to activate the digital controller. Typical vibration and pressure spectra taken at a flow velocity of 21 m/s are shown in Figure 7(a). Interestingly, the system response with the controller activated by the vibration signal is very similar to that obtained by the narrow-band controller, see Figure 6(b). As can be seen in Table 1, the spectral peak amplitude of vibration is reduced by 31 dB and the overall r.m.s. amplitude by 30 dB. However, the pressure oscillation is simply shifted to a higher frequency without much reduction in its amplitude (only about 7 dB reduction). This higher frequency of pressure oscillation corresponds to the natural frequency of the jet-'rigid' edge oscillator, as can be seen from the solid line in Figure 4(b) near $V = 21$ m/s. Further reductions in the pressure amplitude could not be achieved when the vibration signal activated the controller. Seemingly, this is because the wedge response, which is used to activate the controller, is very weak at this "higher" frequency, in comparison to the original vibration amplitude. Moreover, this new oscillation frequency is close to the resonance frequency of the wedge-rocking mode, which is at about 140 Hz. This latter feature must have contributed to the controller inability to further attenuate this new higher-frequency component of the pressure.

The above findings indicated that better attenuation by means of the adaptive digital controller might be attained if the pressure signal, instead of the vibration signal, is used to activate the controller. This is because the pressure signal always reflects the status of the jet oscillation, which is the excitation source, whether it is generating non-resonant jet-edge oscillation or resonant, lock-in vibration.

Typical results of feedback control with the pressure signal activating the adaptive digital controller are given in Figure 7(b) and Table 1. The spectral peaks of the wedge vibration and the pressure oscillation are reduced by 33 and 32 dB, respectively, and the corresponding reductions in the overall r.m.s. amplitudes are 31 and 21 dB. With feedback

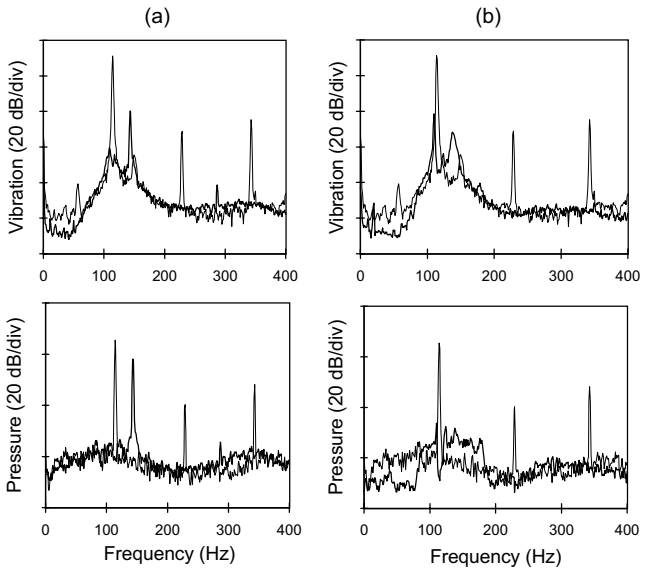

Fig. 7. Typical results showing the effect of the adaptive digital controller on the lock-in wedge vibration; $V = 21$ m/s; (a) Controller activated by the *wedge vibration* signal; (b) by the *pressure* signal. Upper figures: wedge vibration; lower figures: pressure spectra.

TABLE 1

Reductions in the amplitudes of the spectral peaks and the overall rms amplitudes caused by the adaptive digital controller

	Measured variable	Controller activated by vibration signal (dB)	Controller activated by pressure signal (dB)
Wedge vibration	Amplitude of spectral peak	31	33
	Overall r.m.s. amplitude	30	31
Pressure oscillation	Amplitude of spectral peak	7·4	32
	Overall r.m.s. amplitude	6·7	21

control, the pressure spectrum does not contain any narrow band excitation, and the vibration spectrum reflects the wedge response, at its resonance frequencies, to broadband excitation by the impinging jet.

Flow visualization photographs taken without and with feedback control are shown in Figure 8. The top photograph corresponds to system oscillations within the lock-in range without control ($V = 21$ m/s). The middle photograph shows the effect of feedback control when the digital controller was activated by the vibration signal. The upper time signal illustrates that the wedge vibration has vanished. However, the jet and the pressure signal continue to show unsteady activities, albeit with less intensity. The oscillation frequency with control (the middle photo) is clearly seen to be higher than that without control (the top photo). The bottom photograph was taken when the controller was activated with the pressure signal. The jet structure and the time signals show no signs of organized oscillations at all, indicating complete suppression of narrow-band vibration and noise. These visualization photographs elucidate the physical mechanisms already discussed in conjunction with the spectra of Figure 7.

The excellent performance achieved when the pressure signal was used for control has two reasons. First, as mentioned earlier, the controller is activated by the signal which represents the response of the excitation source. Secondly, the jet oscillation pattern, here antisymmetric,[†] is the same for *both the resonant (*i.e. *the lock-in) and the nonresonant cases*. Thus, when the two sets of speakers are connected to operate out-of-phase with each other, the active feedback matches the jet oscillation pattern occurring during both the resonant and the non-resonant oscillations. These phase relations are different from those reported by Ziada (2001) for the case of acoustic resonance of a deep cavity excited by a similar jet impinging on a slot. In that case, the jet switched its oscillation pattern from symmetric to antisymmetric as the system progressed from non-resonant to "acoustic" resonance oscillations. Due to this mode switching, feedback suppression of acoustic resonance within the lock-in range was more difficult and less effective than in the present case of structural resonance.

5. CONCLUSIONS

In order to investigate the effect of feedback control on the coupling mechanism between a fluid-dynamic oscillator and a structural resonator, an experimental set-up has been

[†]The terminology symmetric and antisymmetric modes of jet oscillation refers to whether the vortices at both sides of the jet are formed in a symmetric or alternating pattern, with respect to the jet centerline. This is somewhat analogous to symmetric and alternating vortex shedding from bluff bodies in cross flow. More details can be found in Ziada (1995, 2001).

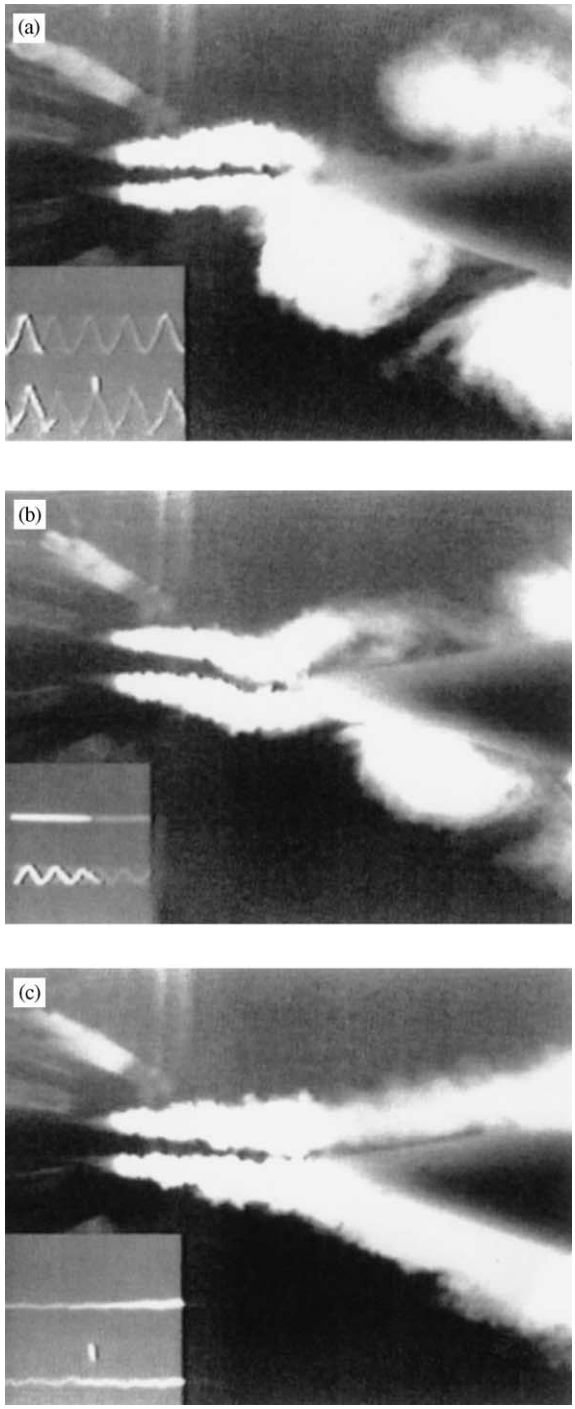

Fig. 8. Flow visualization photographs showing (a) original flow structure without control; (b) flow structure under feedback control with the vibration signal activating the digital controller; (c) same as in (b) but controller activated by the pressure signal.

carefully designed. This set-up consisted of a planar jet impinging upon a flexible wedge and generated strong lock-in vibration over a wide range of flow velocity. Within the lock-in range, the oscillation frequency was determined by the wedge resonance frequency and therefore it deviated substantially from the natural frequency of the fluid-dynamic oscillator, i.e. the "jet-edge oscillator".

An adaptive digital controller was used to activate loudspeakers focused on the jet exit only to counteract the upstream feedback resulting from the *wedge vibration*. When the *vibration signal* was used to activate the controller, the wedge vibration was substantially reduced, but the impinging jet continued to oscillate at a higher frequency approximating the natural frequency of the jet-edge oscillator. This resulted in only slight reduction in the pressure amplitude. However, when the *pressure signal* was used to activate the controller, both the vibrations and the pressure pulsations were entirely suppressed without destabilizing other modes of oscillation.

ACKNOWLEDGEMENTS

The experiments reported upon in this paper were carried out at *Sulzer Innotec* in Switzerland before the author joined McMaster University. The help of Mr E. Jud in the course of measurements and the financial support from *Sulzer Innotec* and the Swiss National Energy Research funds are gratefully acknowledged.

REFERENCES

BAZ, A., & RO, J. 1991 Active control of flow-induced vibrations of a flexible cylinder using direct velocity feedback. *Journal of Sound and Vibration* **146,** 33–45.

CATTAFESTA III, L.N., GARG, S., CHOUDHARI, M., & LI, F. 1997 Active control of flow-induced cavity resonance. AIAA paper 97-1804. Washington, DC: AIAA.

FFOWCS WILLIAMS, J.E., & HUANG, X.Y. 1989 Active stabilization of compressor surge. *Journal of Fluid Mechanics* **204,** 245–262.

GOPALKRISHNAN, R., TRIANTAFYLLOU, M.S., TRIANTAFYLLOU, G.S., & Barrett, D. 1994 Active vorticity control in a shear flow using a flapping foil. *Journal of Fluid Mechanics* **274,** 1–21.

HUANG, X.Y., & WEAVER, D.S. 1991 On active control of shear layer oscillations across a cavity in the presence of pipeline acoustic resonance. *Journal of Fluids and Structures* **5,** 207–219.

MCGRATH, S., & SHAW, L. 1996 Active control of shallow cavity acoustic resonance. *Proceedings of 27th AIAA Fluid Dynamics Conference*, June 17–20 New Orleans, LA, USA

NAKANO, M., & ROCKWELL, D. 1993 The wake from a cylinder subjected to amplitude-modulated excitation. *Journal of Fluid Mechanics* **247**, 79–110.

NAUDASCHER, E., & ROCKWELL, D. 1994 *Flow-Induced Vibrations: An Engineering Guide*. Rotterdam: A.A. Balkema.

POWELL, A. 1961 On the edge-tone. *Journal of the Acoustical Society of America* **33,** 9–19.

ROCKWELL, D., & NAUDASCHER, E. 1979 Self-sustained oscillations of impinging shear layers. *Annual Review of Fluid Mechanics* **11,** 67–94.

ROCKWELL, D. 1992 Active control of globally unstable separated flows. In *Proceedings of International Symposium on Unsteady Fluid Dynamics* (eds J. A. Miller & D. P. Telionis), FED-Vol. 92, pp. 379–394, Toronto, Canada. New York: ASME.

SARNO, R.L., & FRANKE, M.E. 1994 Suppression of flow-induced pressure oscillations in cavities. *Journal of Aircraft* **31,** 90–96.

WELSH, M.C., HOURIGAN, K., ALFREDSON, R.J., & LIN, P. 1991 Active control of flow-excited acoustic resonance: higher order acoustic modes. In *Proceedings of International Conference on Flow-Induced Vibration*, Brighton, England. I.Mech.E. Publication no. 1991-6, pp. 531–528.

WILTSE, J.M., & GLEZER, A. 1993 Manipulation of free shear flows using piezoelectric actuators. *Journal of Fluid Mechanics* **249,** 261–285.

ZIADA, S. 1995 Feedback control of globally unstable flows: impinging flows. *Journal of Fluids and Structures* **9,** 907–923.

ZIADA, S. 1999 Feedback control of flow-excited cavity resonance. In *Flow-Induced Vibration-1999*, (ed. M.J. Pettigrew), PVP-Vol. 389, pp. 325–330, ASME: New York.

ZIADA, S. 2001 Interaction of a jet-slot oscillator with a deep cavity resonator and its control. *Journal of Fluids and Structures* **15**, 831–843.

ZIADA, S., & ROCKWELL, D. 1982 Self-excited oscillations of a mixing layer-wedge system. *Journal of Fluid Mechanics* **124,** 307–334.